

THERMAL STABILITY OF AMINO ACID-(TYROSINE AND TRYPTOPHAN) COATED MAGNETITES

L. Patron¹, G. Marinescu¹, D. Culita¹, L. Diamandescu² and O. Carp^{1*}

¹Institute of Physical Chemistry 'Ilie Murgulescu', Splaiul Independentei, No. 202, 060021, Bucharest, Romania

²Institute of Atomic Physics, National Institute of Material Physics, P.O.Box MG-7, 76900, Bucharest, Romania

The thermal stability of two amino acid-(tyrosine and tryptophan) coated magnetite and their corresponding precursors, $[Fe_2^{III}Fe^{II}(Tyr)_8]9H_2O$ and $[Fe_2^{III}Fe^{II}(Trp)_2(OH)_4](NO_3)_2\cdot8H_2O$ (where tyrosine=Tyr and tryptophan=Trp), was analyzed in comparison with free amino acids. The complexes present a lower thermal stability relative to the free ligand, due to the catalytic effect introduced by the iron cation and the presence of NO_3^- groups. The presence of NO_3^- group determines also a different degradation's stoichiometry of the amino acid anion comparative with the one expressed by the free ligand molecule. The amino acid bonded to magnetite decomposes in two steps, its presence inducing an increasing of $\gamma-Fe_2O_3 \rightarrow \alpha-Fe_2O_3$ conversion temperature.

Keywords: amino acid-coated magnetite, thermal analysis, tryptophan, tyrosine

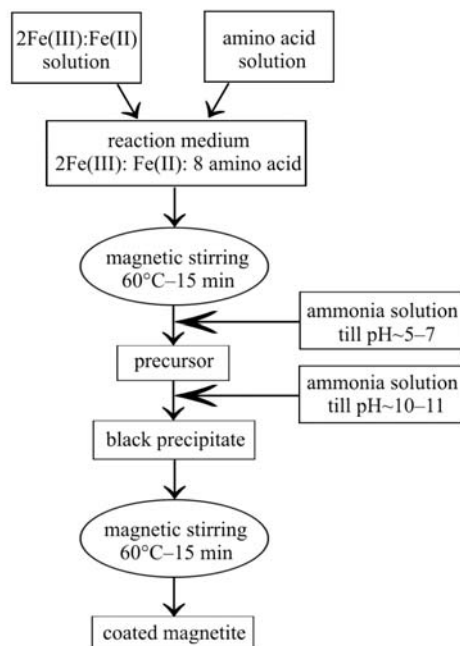
Introduction

Thermal investigations plays an important role in the exploration of materials with applications in the medicine field (therapeutic and diagnostic uses) [1–3]. Magnetite nanoparticles ranging from 1 to 20 nm have attracted much attention because of their current and potential medical applications [4, 5]. For both, in vivo and in vitro applications, to surround the magnetite particles and to prevent aggregations [6–8], well defined organic coatings are required. Amino acids may represent an appropriate choice due to their high chelating capacity (the presence of amino and carboxyl groups), and non-toxicity.

The present study investigates the thermal behaviour of two coated magnetite with amino acids, namely tyrosine (Tyr) and tryptophan (Trp). Their thermal behaviour is analyzed in comparison with the free amino acids and magnetite's precursors. A decomposition mechanism is proposed. As far as we know, the present paper is the first study in this topic.

Experimental

Synthesis: the used raw materials are $FeSO_4\cdot7H_2O$ (Merck, r.g.), $Fe(NO_3)_3\cdot9H_2O$ (Merck, r.g.), tyrosine (Merck, r.g.), tryptophane (Merck, r.g.) and, ammonium hydroxide solution (28–30%, Reactivil, p.a.). The synthesis pathway is presented in Scheme 1. In aqueous solution, in the presence of Fe^{3+} and Fe^{2+} , the amino acids



Scheme 1 Flow chart of precursors, and magnetite-coated synthesis

form polynuclear coordination compounds species which are dependent on the pH medium. At pH~5, the isolated compounds are $[Fe_2^{III}Fe^{II}(Tyr)_8]9H_2O$ (I) and $[Fe_2^{III}Fe^{II}(Trp)_2(OH)_4](NO_3)_2\cdot8H_2O$ (II). At pH>10, the final obtained compounds are the modified magnetites. The coordination compounds were identified by quantitative analysis. The iron content was de-

* Author for correspondence: carp@apia.ro

terminated by a gravimetric technique, and, the carbon, nitrogen and hydrogen contents by a combustion method on a Carbo Erba Model 1108-CHNS-O elemental analyser. $\text{Fe}_3\text{C}_{72}\text{H}_{98}\text{N}_8\text{O}_{33}$ (I), found (%) / calculated (%): Fe, 8.99/9.49; C, 48.77/48.81; H, 5.47/5.54; N, 6.85/6.36. $\text{Fe}_3\text{C}_{22}\text{H}_{42}\text{N}_6\text{O}_{22}$ (II), found (%) / calculated (%): Fe, 18.72/18.46; C, 29.66/20.01; H, 3.96/4.60; N, 8.86/9.23.

Structure investigations: The FTIR investigations were performed on BIO-RAD FTIR 125 type spectrophotometer in KBr pellets and the X-Ray analysis on a Rigaku-Multiflex diffractometer, using CuK_α . Mössbauer spectra of the two precursors were recorded at room temperature by means of a standard constant acceleration spectrometer with a ^{57}Co diffused in rhodium matrix.

Thermal investigations: were carried under static air, with sample mass about 40 mg at heating rates of 5 K min⁻¹. DSC measurements were performed on a Netzsch thermobalance STA 409 PC/PG type and DTA ones on a Q-1500 D Paulik-Paulik-Erdey derivatograph.

Results and discussions

Characterization of precursors and coated magnetite

Comparing the FTIR spectra of free amino acids, magnetites' precursors and coated a number of changes are clearly evidenced. Figure 1 presents the FTIR spectra of tryptophan system. In precursors spectra (1-b) the most noticeable changes are the disappearance of the C=O stretching band at around

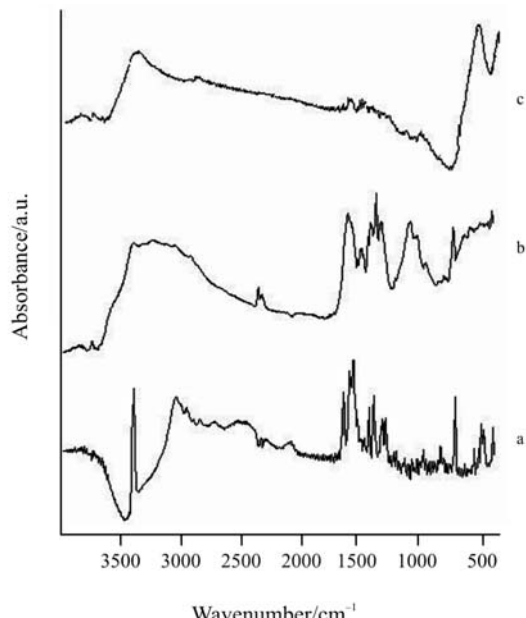


Fig. 1 FTIR spectra of a – triptophan, b – coordination compound $[\text{Fe}^{\text{III}}_2\text{Fe}^{\text{II}}(\text{Trp})_2(\text{OH})_4](\text{NO}_3)_2 \cdot 8\text{H}_2\text{O}$ (II) and c – triptophan-coated magnetite

1580 cm⁻¹ and the appearance of two additional bands which assigned to the asymmetric (ν_{OCOasym}) and symmetric (ν_{OCOsym}) stretching vibrations from the carboxyl anion (~1615 and ~1430 cm⁻¹). The magnitude of $\Delta\nu$ ($\Delta\nu = \nu_{\text{OCOasym}} - \nu_{\text{OCOsym}}$) separation is typical for unidentate coordination of COO^- groups [9]. These vibrational bands are also present in the spectrum of the magnetite (1-c) alongside of the strong band at around 580 cm⁻¹, characteristic to the stretching modes of the Fe–O bond. This fact indicates that a part of amino acids remains chemisorbed onto the surface of the magnetite nanoparticles. The XRD patterns of the coated-magnetite evidence the presence of clean Fe_3O_4 (Fig. 2), with a value of the mean crystallite size of 120 Å for both studied coated-magnetite.

Figure 3 shows the transmission Mössbauer spectra of the two precursors. As it can be observed

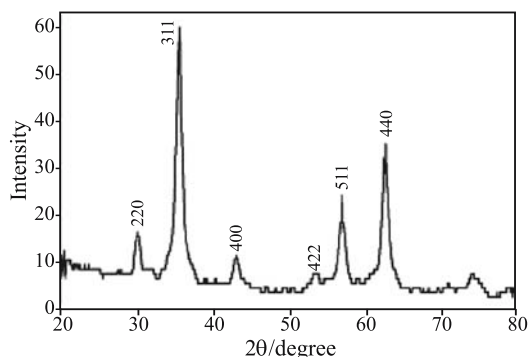


Fig. 2 XRD pattern of triptophan-coated magnetite

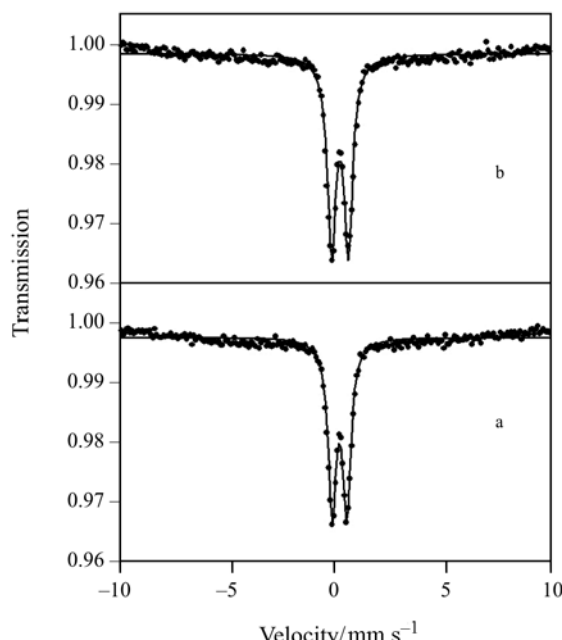


Fig. 3 Room temperature Mössbauer spectra of precursors: a – P1 (tyrosine) and b – P2 (tryptophan). Continuous line is the fit with Lorentzian lines

the spectra consist in quadrupolar doublets. In the case of sample tyrosine precursor (I) the quadrupolar splitting (QS) is about 0.67 ± 0.02 mm s $^{-1}$ and the isomer shift (IS)= 0.29 ± 0.01 mm s $^{-1}$. These parameters support the presence of the high spin state Fe $^{3+}$ in distorted octahedral symmetry. The Mössbauer hyperfine parameters for the tryptophan precursor (II), QS= 0.77 ± 0.02 mm s $^{-1}$ and IS= 0.31 ± 0.01 mm s $^{-1}$ are close to those of the tyrosine one; however the local symmetry at the iron ions seems to be more distorted than in the (I) sample. In both cases the line widths are close to the α -Fe calibration foil that means no other doublets can be considered in the computer fit run.

Thermal behaviour of tyrosine compounds

The thermal decomposition of free tyrosine occurs through two stages in the temperature range 196–640°C (Fig. 4, Scheme 2). The first one (196–338°C) is a complex one, consisting in at least two decomposition steps, identified by the presence of two maxima on DTG curve (262 and 273°C). The first one may be assigned to the formation of *p*-hydroxy benzoic acid and the second to the phenol formation (Scheme 2). The experimental/theoretical values of the mass losses of the first stage are close (calcd./found: 43.98/44.52%). Taking into consideration the usual degradation route of amino acids, the development of

the unstable intermediate 3-(*p*-hydroxyphenyl)-2 ceto-propionic acid can not be ignored. Its presence, will be confirmed or not in further investigations. This decomposition stage is associated with the presence of a weak exothermic effect ($T_{\max \text{DTA}}=263^\circ\text{C}$) followed by a weak endothermic one ($T_{\max \text{DTA}}=270^\circ\text{C}$). Such behaviour may be explained as follows: the thermal degradation and the melting of the amino acid molecule are two partially overlapped processes. If in the first temperature range the oxidative degradation of the amino acid represents the dominant process, in the second prevails the endothermicity of the melting. The next exothermic decomposition stage occurs in a large temperature range (338–640°C) representing the decomposition of the phenol (calcd./found: 56.02/55.68%).

The corresponding polynuclear coordination compound $[\text{Fe}_2^{\text{III}}\text{Fe}^{\text{II}}(\text{Tyr})_8]9\text{H}_2\text{O}$ (I) underwent a three-step decomposition in the temperature range 106–555°C (Fig. 5, Scheme 3). The observed mass loss (86.47%) is in good agreement with the calculated one (86.46%), considering as end product $\alpha\text{-Fe}_2\text{O}_3$. The first decomposition step (111–211°C) associated with an endothermic effect represents the evolving of five water molecules (calcd./found: 5.13/5.14%). The second one, connected with a weak exothermic effect, corresponds to the evolving of the remainder four water molecules and onset of the degradative

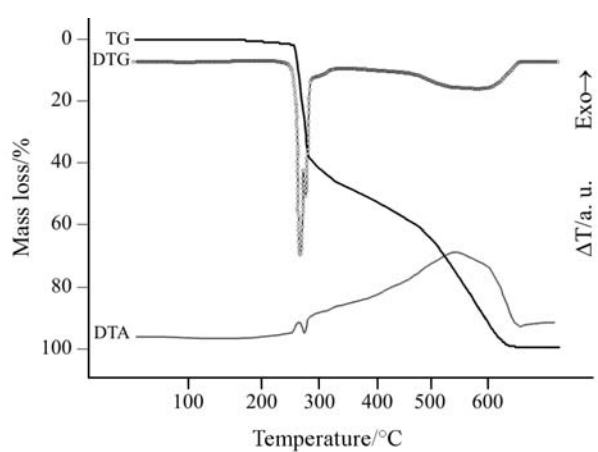


Fig. 4 TG, DTG and DTA curves of free tyrosine (Tyr) (heating rate 5°C min $^{-1}$)

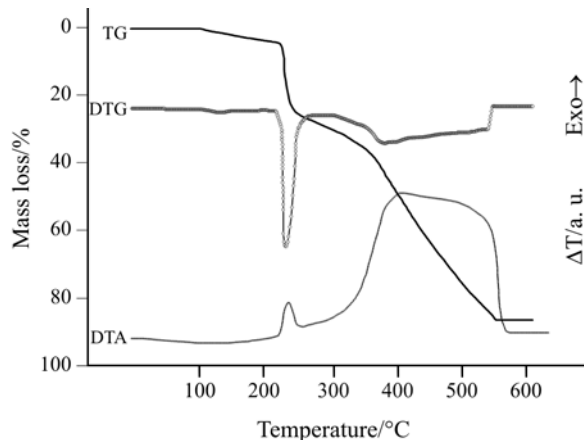
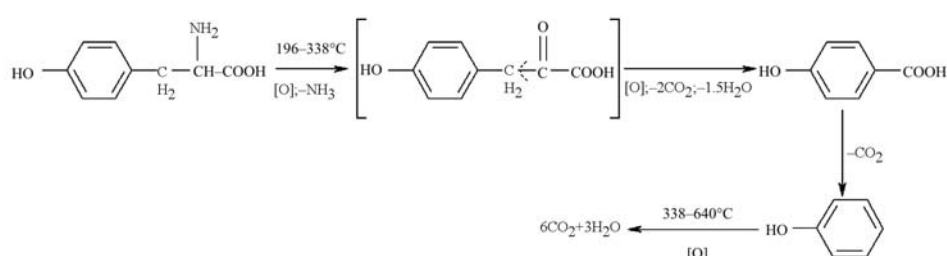
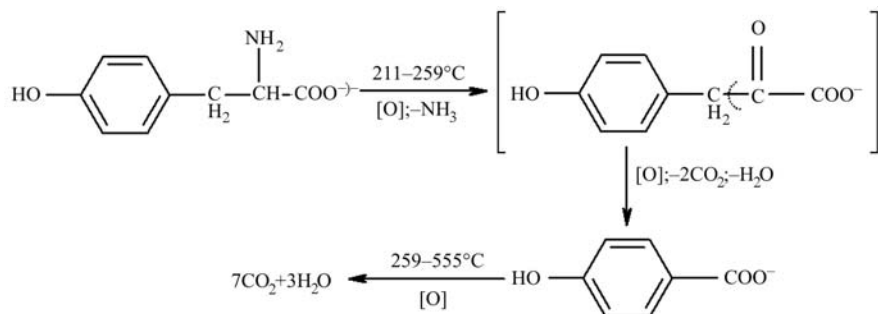


Fig. 5 TG, DTG and DTA curves of $[\text{Fe}_2^{\text{III}}\text{Fe}^{\text{II}}(\text{Tyr})_8]9\text{H}_2\text{O}$ (I) compound (heating rate 5°C min $^{-1}$)



Scheme 2 Proposed decomposition pathway for tyrosine free ligand



Scheme 3 Proposed decomposition pathway for tyrosine anion ligand of the coordination compound $[\text{Fe}^{\text{III}}_2\text{Fe}^{\text{II}}(\text{Tyr})_8]9\text{H}_2\text{O}$

oxidation of the tyrosine ligand with formation of *p*-hydroxy benzoate anion (calcd./found: 19.57/19.67%). As in the case of tyrosine decomposition the formation of the unstable intermediate 3-(*p*-hydroxyphenyl)-2 keto-propionate can not be ignored. The last decomposition step (259–555°C) represents the decomposition of *p*-hydroxy benzoate anions with a simultaneously oxidation of Fe^{II} to Fe^{III} (calcd./found: 61.64/61.65%). Different from the tyrosine decomposition, the decomposition step is limited to the formation of *p*-hydroxy benzoate. A single maximum of the DTG curve located at lower temperature comparative with free tyrosine ones (230°C comparative with 262°C) is identified. The final decomposition temperature of the coordination compound lower with 85°C than that detected for tyrosine (555°C comparative with 640°C), denotes a catalytic effect of iron cations upon the thermal decomposition of amino acid anion.

The tyrosine coated magnetite underwent a three stepped decomposition (Fig. 6). The first endothermic step (32.4–139.3°C, $T_{\max \text{ DTG}}=54.0^\circ\text{C}$, $\Delta H=-80.13$), corresponds to water elimination (mass loss 1.75%). The dehydrated magnetite is stable till 246.8°C when the degradation of amino acid commences. Two distinct temperature intervals are detected for the amino acid de-

composition: 246.8–356.8°C (mass loss 0.58%) and 566.8–596.8°C (mass loss 0.16%), temperatures close with those find out in the decomposition of the corresponding precursor. Because no characteristic peak for Fe^{2+} to Fe^{3+} oxidation is evidenced on DSC curve, two assumptions may be advanced: the oxidation occurs either during the first temperature range of tyrosine evolving, or gradual, in a wide-ranging temperature interval. The relative intense exothermic peak with $T_{\max \text{ DSC}}=582.3^\circ\text{C}$ ($\Delta H=89.25 \text{ J g}^{-1}$), is attributed to $\gamma\text{-Fe}_2\text{O}_3 \rightarrow \alpha\text{-Fe}_2\text{O}_3$ transformation. It is worth to be mentioned the high temperature of the iron oxides conversion, such conversion occurring usually at ~ 400 –450°C [10, 11].

Thermal behaviour of tryptophan compounds

The thermal decomposition of free tryptophan (Fig. 7, Scheme 4) occurs in the temperature range 218–710°C through three distinct decomposition stages. The first decomposition stage (218–270°C) in which two maxima of the DTG is registered (243 and 250°C) represents the oxidative breaking of the side chain, with the formation of 1-indol-3 carboxylic acid and 1-indol-3-yl acetic acid as intermediates (calcd./found: 20.77/20.87%, Scheme 3). The decomposition stage is associated with the presence of a weak exothermic effect ($T_{\max \text{ DTA}}=253^\circ\text{C}$) followed by a weak endothermic one ($T_{\max \text{ DTA}}=258^\circ\text{C}$). As in the tyrosine decomposition, this is explained by a partially overlapping of the degradative decomposition and melting of the organic compound. Similar with tyrosine degradation, the initial development of a keto acid due to an oxidative deamination is proposed. The next decomposition step (270–438°C) represents the decarboxylation of the acid with formation of the indol molecule (calcd./found: 19.63/21.25%), which decomposes on further heating (483–710°C, calcd./found: 57.00/57.88%).

The second coordination compound, $[\text{Fe}^{\text{III}}_2\text{Fe}^{\text{II}}(\text{Trp})_2(\text{OH})_4](\text{NO}_3)_2 \cdot 8\text{H}_2\text{O}$ (II) suffers a five-stage decomposition, one endothermic and four exothermic, in the temperature range 61–659°C

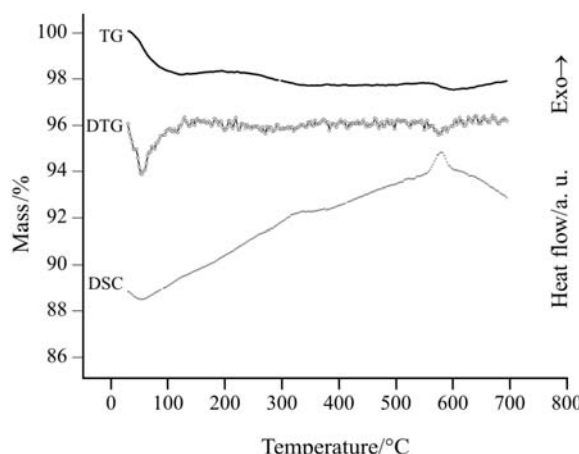


Fig. 6 TG, DTG and DSC curves of tyrosine-coated magnetite (heating rate 5°C min^{-1})

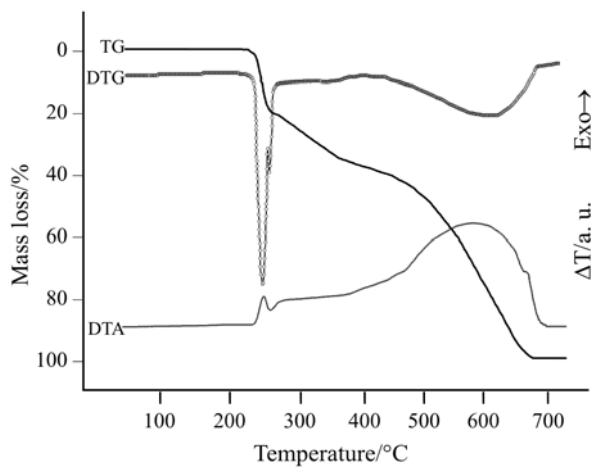
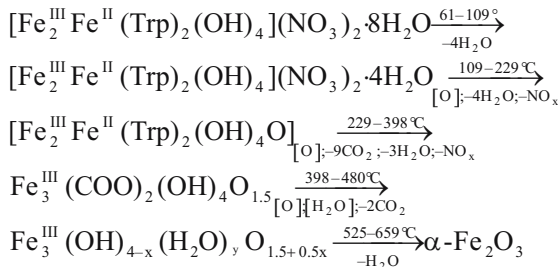


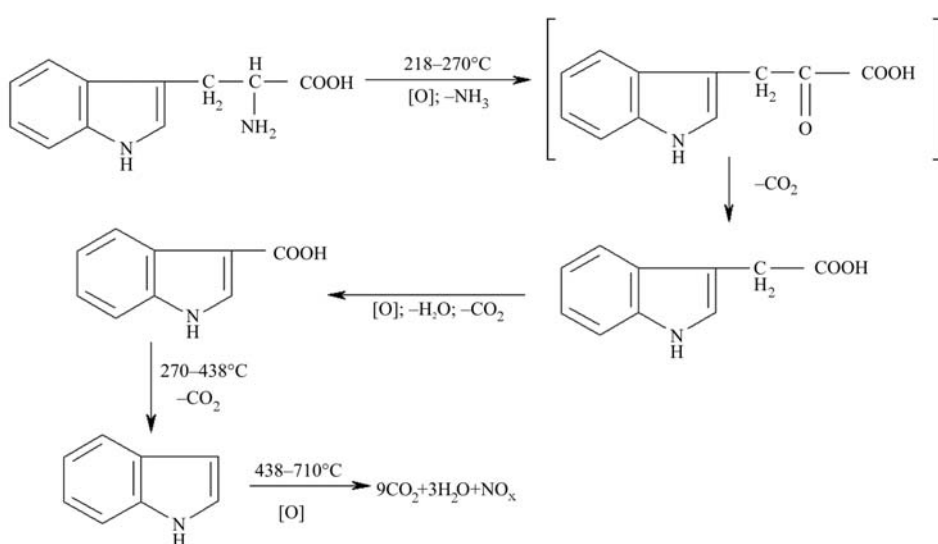
Fig. 7 TG, DTG and DTA curves of free tryptophan (Trp) (heating rate $5^{\circ}\text{C min}^{-1}$)

(Fig. 8). The experimental mass loss assuming $\alpha\text{-Fe}_2\text{O}_3$ formation is in agreement with the theoretical mass loss (calcd./found: 73.13/73.89%). The first weak endothermic decomposition step ($61\text{--}109^{\circ}\text{C}$), represents the evolving of four water molecules (calcd./found: 7.84/8.12%). The next decomposition step ($109\text{--}229^{\circ}\text{C}$) may be assigned to the simultaneously evolving of remaining water molecules and NO_3^- groups (calcd./found: 18.95/19.61%). From now on, the progress of the decomposition occurs completely differently comparative with the free ligand amino acid. On further heating ($229\text{--}398^{\circ}\text{C}$), the breaking down of tryptophan anion skeleton occurs, accompanied by the oxidation of Fe^{2+} to Fe^{3+} (calcd./ found: 34.65/33.17%). The stoichiometric calculation and the preserving in the FTIR spectra of the isolated reaction intermediate of ν_{OCOasym} and ν_{OCOsym} bands (1608 and

1390 cm^{-1}) lead to a decomposition intermediate of $\text{Fe}_3(\text{COO})_2(\text{OH})_4\text{O}_{1.5}$ composition. The following two decomposition steps ($398\text{--}480$ and $525\text{--}659^{\circ}\text{C}$) are assigned to the formation of an aqua-hydroxo complex of molecular formula $\text{Fe}_2(\text{OH})_{4-x}(\text{H}_2\text{O})_y\text{O}_{1.5+0.5x}$ (found mass loss: 9.48%) and $\alpha\text{-Fe}_2\text{O}_3$ (found mass loss: 4.06%). The formation of aqua-hydroxo complex as intermediates during the decomposition of coordination compounds containing mono or poly (hydroxy) carboxylic acid anions or amino acids as ligands [10, 12]. The final decomposition temperature of the coordination compound is lower with $\sim 50^{\circ}\text{C}$ in respect with the free tryptophane.



The thermal behaviour of tryptophan-coated magnetite is similar with that of the tyrosine modified magnetite (Fig. 9). A first endothermic step ($32.5\text{--}121.0^{\circ}\text{C}$, $T_{\max \text{ DTG}}=53.5^{\circ}\text{C}$, mass loss 2.51%, $\Delta H=-81.92$) corresponding to water evolving, is followed by amino acid two-stepped degradation ($148.5\text{--}361.0$ and $498.5\text{--}538.5^{\circ}\text{C}$, mass losses 1.28 and 0.15%). The lower mass loss comparative with the tyrosine similar compound registered in the second temperature range, may be responsible to the decrease of the $\gamma\text{-Fe}_2\text{O}_3 \rightarrow \alpha\text{-Fe}_2\text{O}_3$ conversion temperature ($T_{\max \text{ DSC}}=524.5^{\circ}\text{C}$, $\Delta H=141.5\text{ g}$).



Scheme 4 Proposed decomposition pathway for tryptophan free ligand

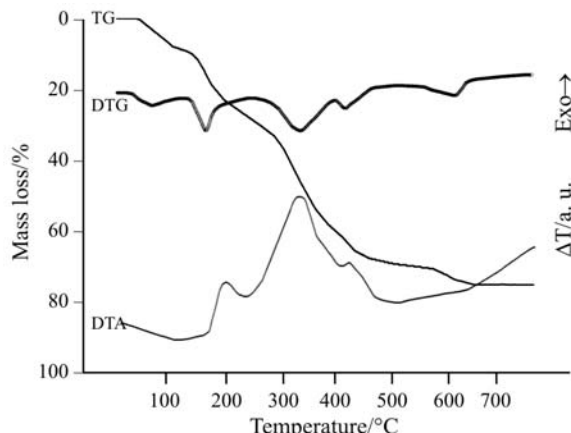


Fig. 8 TG, DTG and DTA curves of $[\text{Fe}_2^{\text{III}} \text{Fe}^{\text{II}} (\text{Trp})_2(\text{OH})_4]^2(\text{NO}_3)_2 \cdot 8\text{H}_2\text{O}$ (II) compound (heating rate 5°C min^{-1})

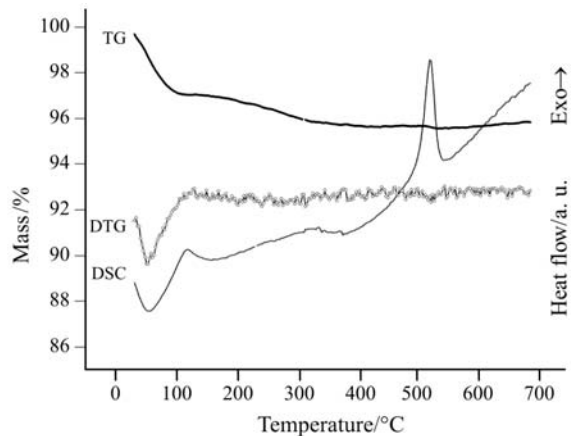


Fig. 9 TG, DTG and DSC curves of tryptophan-coated magnetite (heating rate 5°C min^{-1})

Conclusions

The magnetite coated precursors, $[\text{Fe}_2^{\text{III}} \text{Fe}^{\text{II}} (\text{Tyr})_8]9\text{H}_2\text{O}$, $[\text{Fe}_2^{\text{III}} \text{Fe}^{\text{II}} (\text{Trp})_2(\text{OH})_4]^2(\text{NO}_3)_2 \cdot 8\text{H}_2\text{O}$ are less stable than the free ligands. This behaviour is contrary with the usual one, respective a higher thermal stability of the ligand introduced into complexes (due to its coordination) comparative with corresponding free ligand [13–17]. The lower thermal stability expressed by the complexes than the free ligand, has as principal cause the catalytic effect introduced by the iron cation, and the presence of NO_3^- groups. Additional, the presence of NO_3^- group determines a different stoichiometry degradation of the amino acid anion comparative with the one

expressed by the free ligand molecule. The thermal behaviour of the two coated magnetite is similar, the decompositions taking place in three stages. The evolving of adsorbed water is followed by a two stepped decomposition of the amino acid. The registered $\gamma\text{-Fe}_2\text{O}_3 \rightarrow \alpha\text{-Fe}_2\text{O}_3$ conversion temperature is higher comparative with the one mentioned by the literature, and may be related to the amount of amino acid eliminated in its temperature range of occurrence.

References

- O. Z. Yeşilel and H. Ölmez, *J. Therm. Anal. Cal.*, 86 (2006) 211.
- N. T. Madhu, P. K. Radhakrishnan, E. Williams and W. Linert, *J. Therm. Anal. Cal.*, 79 (2005) 157.
- M. Badea, R. Olar, D. Marinescu, G. Vasile and S. Stoleru, *J. Therm. Anal. Cal.*, 80 (2005) 679.
- A. Ito, M. Shimkai, H. Honda and T. Kobayashi, *J. Biosci. Bioenerg.*, 100 (2005) 1.
- S. Mornet, S. Vasseur, F. Grasset and E. Duguet, *J. Mater. Chem.*, 14 (2004) 2161.
- S. Yu and G. H. Chow, *J. Mater. Chem.*, 14 (2004) 2781.
- N. Fauconnier, J. N. Pons and A. Bee, *J. Colloid Interface Sci.*, 194 (1997) 427.
- M. H. Sousa, J. C. Rubbin and F. A. Tourinho, *J. Magn. Magn. Mater.*, 225 (2001) 67.
- K. Nakamoto, ‘Infrared and Raman Spectra of Inorganic Compounds’, Ed. 4, J. Wiley & Sons, 1986, p. 223.
- O. Carp, L. Patron, L. Diamandescu and A. Reller, *Thermochim. Acta*, 390 (2002) 169.
- N. J. Tang, W. Zhong, H. Y. Jiang, X. L. Wu, W. Liu and Y. W. Du, *J. Mag. Mag.*, 282 (2004) 92.
- O. Carp, D. Gingas, I. Mindru and L. Patron, *Thermochim. Acta* (in press).
- M. Sikorska-Iwan, R. Mrozek and Z. Rzączyńska, *J. Therm. Anal. Cal.*, 60 (2000) 139.
- R. R. Mahajan, P. S. Makashir and J. P. Agrawal, *J. Therm. Anal. Cal.*, 65 (2001) 935.
- I. M. M. Kenawy, M. A. Hafez and R. R. Lashein, *J. Therm. Anal. Cal.*, 65 (2001) 723.
- K. Mészáros Szécsény, V. M. Leovac, Ž. K. Jaćimović and G. Pokol, *J. Therm. Anal. Cal.*, 74 (2003) 943.
- B. N. Sivasankar and L. Ragunath, *Thermochim. Acta*, 397 (2003) 237.

Received: August 29, 2006

Accepted: February 16, 2007

DOI: 10.1007/s10973-006-8082-4